Magnetic anisotropy of ordered and disordered FePd thin films

L. Szunyogh
Department of Theoretical Physics, Budapest University of Technology and Economics, Budafoki út 8, H-1521 Budapest, Hungary and Center for Computational Materials Science, Gumpendorfer Strasse 1a, A-1060 Vienna, Austria

J. Zabloudil, A. Vernes, and P. Weinberger
Center for Computational Materials Science, Gumpendorfer Strasse 1a, A-1060 Vienna, Austria

B. Újfalussy
Research Institute for Solid State Physics and Optics, Hungarian Academy of Sciences, Konkoly-Thege Miklós u. 29-33, H-1121 Budapest, Hungary

C. Sommers
Laboratoire de Physique des Solides, Université de Paris-Sud, 91405 Orsay, France
(Received 11 August 2000; revised manuscript received 6 February 2001; published 17 April 2001)

The magnetic anisotropy energy of Fe films, FePd surface alloys, as well as ordered and interdiffused $(Fe_nPd_m)_r$ superstructures on Pd(100) and Pd(111) are evaluated using a fully relativistic spin-polarized screened Korringa-Kohn-Rostoker method. It is found that only an ordered Fe_1Pd_1 superstructure grown on Pd(100) exhibits perpendicular magnetism, while for all other systems under investigation the magnetization is oriented in plane. By using the inhomogeneous coherent potential approximation for layered systems, the effect of ordering into (repeated) superstructures can be described *ab initio*. It is found that already small amounts of interdiffusion can be decisive for the actual value of the magnetic-anisotropy energy. The present theoretical results as compared to experiments indicate that changes in the magnetic-anisotropy energy related to chemical order might arise either through changes in the crystallographic structure or through changes in the electronic structure and Pd-induced spin-orbit coupling.

DOI: 10.1103/PhysRevB.63.184408 PACS number(s): 75.30.Gw, 75.70.Ak, 75.70.Cn

I. INTRODUCTION

Iron-palladium systems raised early interest as it has been discovered that palladium becomes magnetically active in the presence of magnetic impurities.[1,2] In particular, Fe impurities in bulk Pd showed a high net magnetic moment[3] that has been partially confirmed by first-principles calculations within the local spin-density approximation (LSDA).[4] Later on the atomic, electronic, and magnetic structure of Fe films grown on Pd(111) and Pd(100) have been intensively investigated experimentally.[5–9] Remarkably, ultrathin Fe films on Pd(100) revealed ferromagnetic ordering with the magnetization oriented parallel to the surface when grown at 300 K, while at 100 K a magnetization perpendic ular to the surface was observed for thicknesses up to three monolayers and parallel for larger thicknesses.[6–8] In accordance with these observations, also FePd nanomultilayers showed an increasing tendency towards perpendicular magnetization with decreasing thickness of the Fe layers.[10] However, depending on the growth conditions and the film thickness the atomic structure of the Fe films was predicted to be quite different in different experimental studies;[7,9] even an fcc-like phase of Fe in the nanomultilayers was detected.[10] Furthermore, for Fe/Pd(111) superlattices interatomic diffusion at the interfaces restricted to about three atomic layers has been found to be consistent with x-ray and Mössbauer spectra,[11] while $Fe_8/Pd_n(100)$ multilayers grown by molecular-beam epitaxy are claimed to have nearly perfect interfaces.[12] For Fe films as thin as 1–3 atomic layers on Pd(100), recent experiments[13,14] explored a face-centered-tetragonal (fct) structure related to the in-plane lattice constant of Pd(100), with a corresponding high-spin Fe phase caused by an enlarged atomic volume of Fe. This volume effect has been nicely demonstrated in a previous theoretical work by dos Santos and Kuhnen.[15] Also recently, chemical disorder such as interdiffusion and surface alloying has been understood to influence the perpendicular magnetic anisotropy (PMA) in these systems.[13,16] Especially, for $Fe_{0.5}Pd_{0.5}$ thin films it has been established that only the totally ordered $L1_0$ phase exhibits a PMA.[17,16]

The purpose of this paper is to present a computational study of the magnetic-anisotropy energy (MAE) of Fe films and Fe/Pd superstructures on Pd(100) and Pd(111) focusing mainly on effects of alloying and interdiffusion. The main question to answer is by which mechanism chemical disorder influences the MAE in these systems. In Sec. II we briefly describe the method of our calculations, in Sec. III we present and discuss our results, while in Sec. IV we give a comparison to available experiments and draw our conclusions.

II. COMPUTATIONAL ASPECTS

All calculations were performed using a fully relativistic spin-polarized version of the screened Korringa-Kohn-Rostoker method.[18] In all cases the effective potentials and effective exchange fields were obtained self-consistently based on the exchange-correlation functional given in Ref.

19, by making use of surface Brillouin-zone integrations with $45k_{\|}$ vectors per irreducible wedge (ISBZ), and a ''buffer'' of at least three Pd layers to the semiinfinite Pd substrate. This was indeed necessary since x-ray magnetic circular dichroism studies revealed that Pd atoms carry a magnetic moment up to four layers from the Fe/Pd interface.[12] Similarly, three to four empty sphere layers were treated self-consistently in order to relax the potentials to the ideal vacuum. For describing disorder (alloying, interdiffusion) the coherent potential approximation CPA for layered systems[20] was applied using the same numerical parameters just mentioned. All calculations refer to the experimental lattice spacing ($a_0=7.3530$ a.u.) of a Pd fcc ''parent lattice,''[21] i.e., no layer relaxations were considered although in principle this would be possible.[22] It should be noted that in the case of a Pd(100) substrate the (constant) interlayer spacing (3.6765 a.u.) is substantially shorter than for a Pd(111) substrate (4.2454 a.u.).

According to the magnetic-force theorem the magnetic-anisotropy energy ΔE_a of layered systems, as defined by the difference of the total energy between a uniform in-plane ($\|$) and perpendicular-to-plane ($\perp$) orientation of the magnetization, is approximated within the LSDA by the corresponding band-energy difference

$$\Delta E_a^{\mathrm{LSDA}} = E_b(\|) - E_b(\perp). \tag{1}$$

Although LSDA, in strict sense, merely implies a differential form of the force theorem,[23] many applications in the past proved the usefulness of the approach in Eq. (1). Note that a self-consistent calculation is carried out only for the $\perp$ direction of the magnetization, keeping then the potentials and effective fields fixed when evaluating Eq. (1). For the case of a Fe monolayer on Pd(100) we computed ΔE_a based on self-consistent calculations corresponding to a perpendicular as well as an in-plane orientation of the magnetization; the respective results are 0.133 meV and 0.136 meV. The difference between these two values lies well within the range of the error arising from the Brillouin-zone integration.[18]

If c_α^p denotes the respective concentrations of the constituents A and B in layer p then in terms of the (inhomogeneous) CPA for layered systems[20] ΔE_b is given by

$$\Delta E_b = \sum_{p=1}^{N} \sum_{\alpha=A,B} c_\alpha^p \Delta E_\alpha^p, \tag{2}$$

where the

$$\Delta E_\alpha^p = \int_{\epsilon_b}^{\epsilon_F} \Delta n_\alpha^p(\epsilon)(\epsilon - \epsilon_F) d\epsilon \tag{3}$$

refer to component- and layer-resolved contributions to the grand-potential at $T=0$. In Eq. (3) $\Delta n_\alpha^p(\epsilon)$ is the difference of the component- and layer-projected density of states with respect to the orientation of the magnetization evaluated using $990k_{\|}$ vectors per ISBZ guaranteeing a reliable convergence[18] for ΔE_b, ϵ_b denotes the bottom of the valence band and ϵ_F is the Fermi energy of the nonmagnetic substrate. The Breit interaction missing in the Kohn-Sham-Dirac Hamiltonian is taken into account *a posteriori* by adding the classical magnetic dipole-dipole contribution ΔE_{dd},[18] usually referred to as shape anisotropy, to ΔE_b

$$\Delta E_a = \Delta E_b + \Delta E_{dd}. \tag{4}$$

Note that in the case of disordered systems we used concentration-averaged magnetic moments in the expression of ΔE_{dd} derived in Ref. 18, that is, we neglected all vertex corrections when averaging[24] the product of two single-site quantities such as magnetic moments. It is also important to mention that because of the definition given in Eq. (1) a positive/negative value of the MAE implies perpendicular/in-plane magnetization of the film.

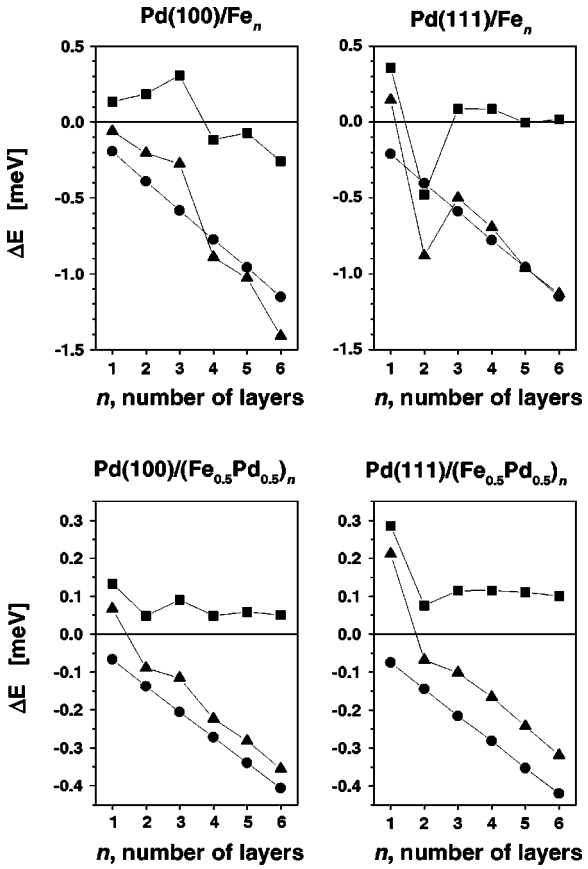

FIG. 1. Band-energy contribution (squares), magnetic dipole-dipole energy contribution (circles) to the MAE and the total MAE (triangles) of pure Fe and disordered $Fe_{0.5}Pd_{0.5}$ films on Pd(100) and Pd(111) substrates. Solid lines serve as a guide for the eye.

III. RESULTS

We first performed calculations for thin Fe films on Pd(100) and Pd(111) substrate. The calculated MAE is depicted in the upper panels of Fig. 1 together with the corresponding band energy and magnetic dipole-dipole contributions. Note that, as will be clear from the figures showing layer-resolved contributions, in our convention the semiinfinite substrate is to the left, therefore, we will write in the following the substrate to the left, i.e., in this case Pd(hkl)/Fe$_n$ with $(hkl)=(100)$ or (111). For Fe films on Pd(100) ΔE_b is positive with an increasing magnitude up to

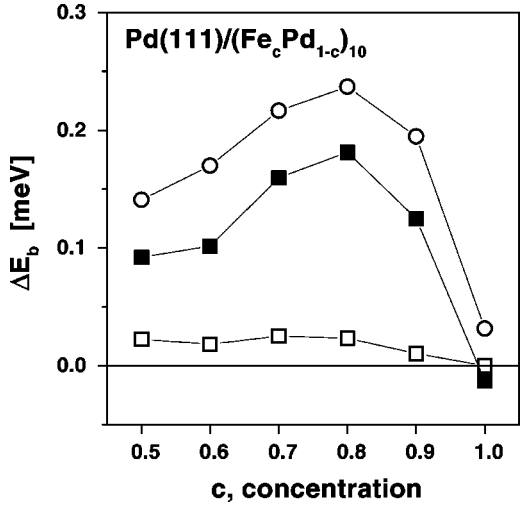

FIG. 2. Band-energy contribution (full squares) to the MAE for disordered $(Fe_cPd_{1-c})_{10}$ films on Pd(111) as a function of the concentration c. The contribution of iron and palladium components in the disordered layers is also displayed as open circles and squares, respectively. Solid lines serve as a guide for the eye.

$n=3$, then changes sign suddenly at $n=4$ and remains negative for thicker films. However, by taking into account the strongly negative magnetic dipole-dipole energy contributions ΔE_{dd}, the theoretical MAE's are negative irrespective of n.

As can be seen from the corresponding entries in Fig. 1 the characteristic differences in the calculated MAE's with respect to the growth direction arise from the differences in the band-energy contributions ΔE_b. In the case of Pd(111)/Fe$_n$ larger variations in ΔE_b can be observed for small n values than for Pd(100)/Fe$_n$: ΔE_b jumps from a positive value at $n=1$ to a large negative value for $n=2$, whereas for $n\geqslant 3$ ΔE_b is slightly positive. From an analysis of layer-resolved contributions of ΔE_b (see Fig. 3) we find that the abrupt decrease of ΔE_b from $n=1$ to $n=2$ is related to the strongly negative band-energy contribution of the subsurface Fe layer. With the exception of $n=1$, by adding ΔE_{dd} to ΔE_b, we again get an in-plane magnetization for Pd(111)/Fe$_n$ films.

Next we compare our results for pure Fe films to those for homogeneously disordered $Fe_{0.5}Pd_{0.5}$ films (lower panels of Fig. 1): for the (100) as well as the (111) growth direction ΔE_b is now positive for all values of n considered, for $n \geqslant 3$ it is larger even than those of the corresponding pure Fe films. Since the average magnetic moment per layer is almost halved as compared to the pure Fe films, ΔE_{dd} is substantially decreased in magnitude. It is, however, large enough to result in an in-plane magnetization for $n\geqslant 2$ for both substrate orientations.

In order to see clearly the effect of alloying we performed calculations for a rather thick film ($n=10$) on Pd(111) by varying the Fe concentration from $c=0.5$ to 1. The band-energy contribution to the MAE is displayed in Fig. 2 together with its componentlike resolution. Note that in this figure the fairly constant contribution of the ''buffer'' Pd layers to ΔE_b are not considered. Apparently, the change of

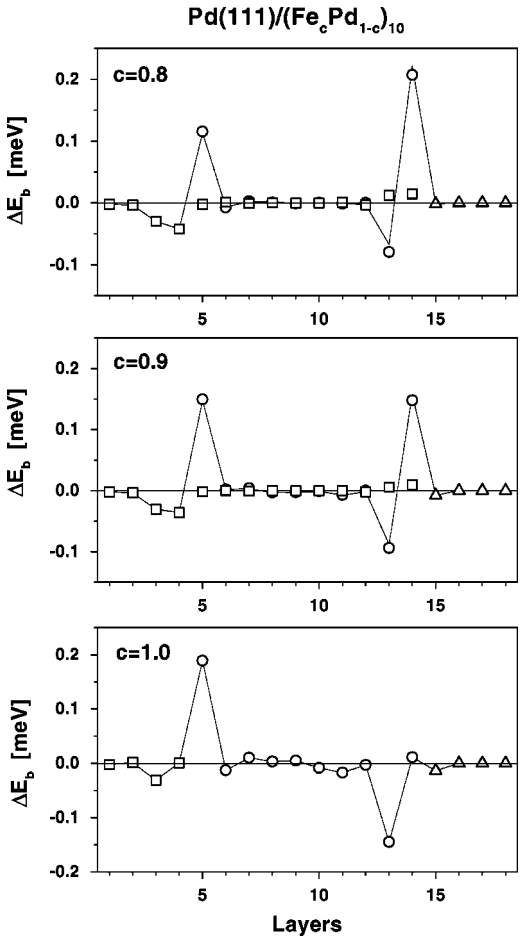

FIG. 3. Layer- and component-resolved contributions (circles, Fe; squares: Pd) to the band-energy part of the MAE in $(Fe_cPd_{1-c})_{10}$ films on Pd(111) for $c=0.8$, 0.9, and 1. The contributions of the ''buffer'' Pd (squares) and empty sphere layers (triangles) are also shown. The thin solid line indicates the shape of the total layer-resolved contributions of ΔE_b. The Pd substrate (origin of counting) is to the left, vacuum to the right.

ΔE_b with respect to the concentration is dominated by the Fe contribution. The nearly linear increase of the ΔE_b of Fe from $c=0.5$ to 0.8 is easy to understand as the amount of Fe is gradually increasing. However, for concentrations larger than 0.8 the ΔE_b of Fe drops dramatically leading to almost negligible contributions at $c=1$, i.e., at the pure Fe-film limit.

The above nontrivial behavior can be understood by further resolving ΔE_b with respect to layers as shown in Fig. 3 for $c=0.8$, 0.9, and 1. As can be seen, the most important contributions to ΔE_b arise from the Fe atoms at the interface and in the two layers next the surface, whereas buried layers do not play a role in the actual size of the MAE. As discussed in Ref. 26 this is a direct consequence of the nearly cubic ''local symmetry'' in such layers. Interestingly, the Pd buffer layers have non-negligible contributions to the MAE. The ΔE_b of Fe at the interface decreases monotonically with the concentration of the Fe component and, thus, cannot explain the anomalous behavior of ΔE_b for $0.8<c<1$. Pronounced changes with c in the contributions of Fe to ΔE_b

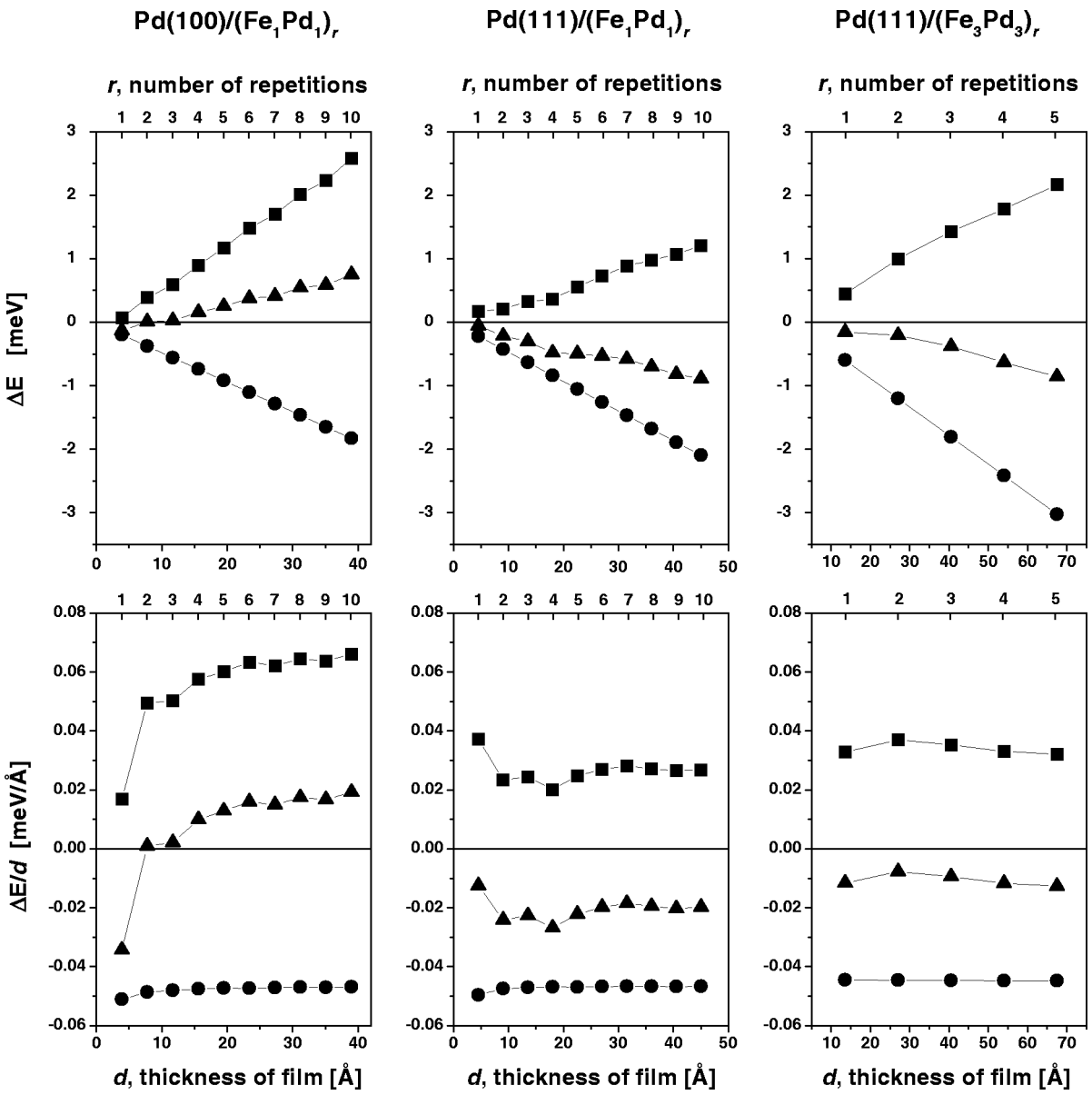

FIG. 4. Upper panels: Band-energy contribution (squares), magnetic dipole-dipole energy contribution (circles) to the MAE and the total MAE (triangles) of ordered FePd superstructures. Lower panel: the same quantities as in the upper panel, however, divided by the film thickness. Solid lines serve as a guide for the eye.

can, however, be detected at the surface and subsurface layers. For $c=1$ the subsurface Fe atoms show large negative contributions, whereas the surface Fe atoms have only a tiny positive one. Substituting 10% of the Fe atoms by Pd atoms, the surface Fe atoms immediately show large positive ΔE_b, while the magnitude of the negative contribution of the subsurface Fe atoms simultaneously decreases. This effect is still increased for a 20% substitution of Fe atoms by Pd. Thus, increasing the Pd concentration, the abrupt increase of ΔE_b can be directly related to changes in the electronic structure of the surface Fe atoms. A possible mechanism might be associated with spin-orbit coupling of the Fe atoms induced by an increasing amount of surrounding Pd atoms (a systematic study of this effect can be found in Ref. 25).

We turn now to the investigation of Pd(hkl)/($\mathrm{Fe}_n\mathrm{Pd}_m$)$_r$ multilayers, that is, multilayers consisting of a number of r repetitions of units built up from n Fe and m Pd layers deposited on a Pd(hkl) substrate. Consequently, such a film is built up from $N=r(n+m)$ atomic layers of thickness $d=d_\perp N$, where $d_\perp$ denotes the (uniform) interlayer spacing. Clearly, from the point of view of high-density magnetic-recording media a large PMA is desired, therefore the aim is to maximize the value of the MAE per repetition or per unit thickness

$$k=\lim_{r\to\infty}\Delta E_a(r)/r \quad \text{or} \quad k=\lim_{d\to\infty}\Delta E_a(d)/d. \tag{5}$$

Based on above studies of Fe and ($\mathrm{Fe}_c\mathrm{Pd}_{1-c}$) films the largest positive k has to be expected for small n and m values. Therefore, we restricted ourselves to the cases of $n=1$ and $m=1$ for both Pd(100) and Pd(111) ($1<r<10$), and in

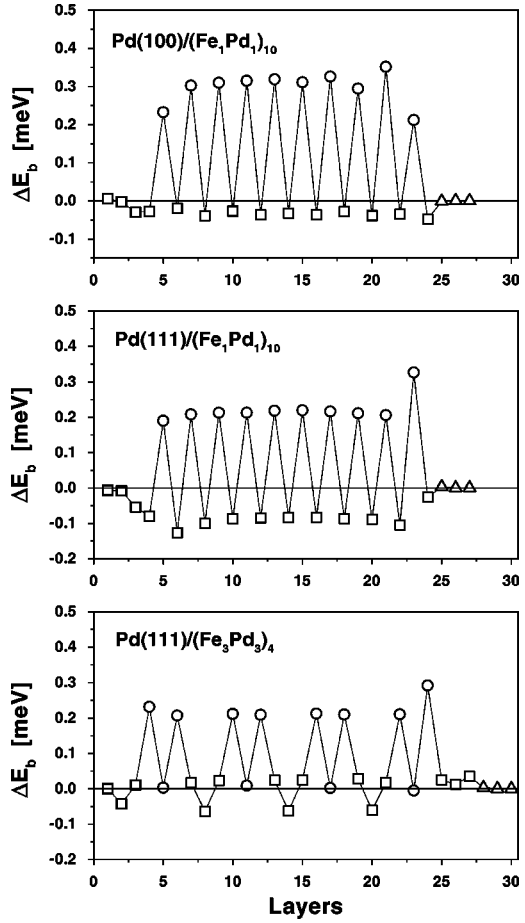

FIG. 5. Layer-resolved contribution (circles, Fe layers; squares, Pd layers) to the band-energy part of the MAE for selected superstructures. In the upper and middle panel the first four and in the lower panel the first three layers correspond to the ''buffer'' Pd layers. Triangles represent the contributions from empty-sphere layers. Thin solid lines serve as a guide for the eye. The Pd substrate (origin of counting) is to the left, vacuum to the right.

order to investigate larger units we also calculated $\mathrm{Pd}(111)/(\mathrm{Fe_3Pd_3})_r$ for $1<r<5$. The corresponding results for the MAE as well as for ΔE_b and ΔE_{dd} with respect to the film thickness (repetitions) are shown in the upper panels of Fig. 4, whereas in the lower panels the same quantities are depicted as normalized to unit thickness. From this figure one can see that although the band-energy contribution to the MAE is positive for each system, only in the case of $\mathrm{Pd}(100)/(\mathrm{Fe_1Pd_1})_r$ it is sufficiently large to keep the MAE positive, whereas superstructures grown on Pd(111) exhibit a negative MAE, i.e., an in-plane magnetization. The k values, Eq. (5), for the MAE that can be read off from Fig. 4 are as follows: $k\simeq 0.02$ meV/Å for $\mathrm{Pd}(100)/(\mathrm{Fe_1Pd_1})_r$, $k\simeq -0.02$ meV/Å for $\mathrm{Pd}(111)/(\mathrm{Fe_1Pd_1})_r$, and $k\simeq -0.013$meV/Å for $\mathrm{Pd}(111)/(\mathrm{Fe_3Pd_3})_r$.

Figure 5 shows the layer-resolved contributions to the ΔE_b for $\mathrm{Pd}(100)/(\mathrm{Fe_1Pd_1})_{10}$, $\mathrm{Pd}(111)/(\mathrm{Fe_1Pd_1})_{10}$, and $\mathrm{Pd}(111)/(\mathrm{Fe_3Pd_3})_4$. A distinct difference between the first two multilayers can be established from inspecting the contributions of the interior Fe layers: they are about 0.3 meV and 0.2 meV, respectively, while those of the interior Pd layers are about -0.03 meV and -0.08 meV, respectively. Concerning the $\mathrm{Pd}(111)/(\mathrm{Fe_3Pd_3})_4$ system it is interesting to note that the innermost Fe layer in each of the $\mathrm{Fe_3}$ slabs has practically a vanishing contribution. On the contrary, the outermost Pd layers of the $\mathrm{Pd_3}$ slabs exhibit a nearly zero ΔE_b^p, whereas the innermost Pd layers retain a ΔE_b^p of about -0.05 meV, indicating that the ''local-symmetry argument'' mentioned above has to be applied with care. As a result a larger k for $\mathrm{Pd}(111)/(\mathrm{Fe_3Pd_3})_r$ is obtained than for $\mathrm{Pd}(111)/(\mathrm{Fe_1Pd_1})_r$ (see Fig. 4).

As already pointed out chemical ordering plays a crucial role for the size of the MAE of Fe/Pd thin films and multilayers. To trace this effect we used a model of interdiffusion for the $(\mathrm{Fe_1Pd_1})_5$ film: in each of the units $\mathrm{Fe_1Pd_1}$ we substituted the same amount of Fe atoms by Pd atoms in the first (originally pure Fe) layer as that of Pd atoms by Fe atoms in the second (originally pure Pd) layer. This leads to a sequence of $(\mathrm{Fe}_c\mathrm{Pd}_{1-c}/\mathrm{Fe}_{1-c}\mathrm{Pd}_c)_5$, which for any c obviously keeps the total amount of Fe and Pd atoms to be fixed. Furthermore, for $c=0.5$ and $c=1$ the homogeneously disordered 50%-50% alloy and the ordered ($L1_0$) superstructure is restored, respectively. For both growth directions, we performed calculations for $0.5\leqslant c\leqslant 1$ simulating thus a continuous transition between the above two limiting cases.

The corresponding results for the MAE are displayed in Fig. 6. As the shape-anisotropy contribution ΔE_{dd} varies only little with c, the variation of the MAE is governed by the corresponding variations of ΔE_b. For the case of films grown on Pd(100) (upper panel of Fig. 6) ΔE_b monotonically decreases with decreasing c. As can be read off from Fig. 6, an interdiffusion of as little as 7% ($c=0.93$) turns the magnetization from out-of-plane to in-plane. Obviously, the decrease of the Fe contribution is ultimately responsible for the decrease of the band-energy part to the MAE as the interdiffusion is increasing. For films grown on Pd(111) (lower panel of Fig. 6) the MAE is negative in the whole range of c, however, a maximum of ΔE_b at about $c=0.9$ can be detected resulting from an interplay of both the Fe and Pd contributions.

In Fig. 7 the layer- and component-resolved contributions to ΔE_b in the above systems are displayed for $c=0.8$, 0.9, and 1. As can be seen from this figure, for the growth direction (100) (left panels) the chemical disorder clearly reduces the ΔE_b of predominantly Fe-like layers, whereas the Fe atoms interdiffused into the Pd layers exhibit an even smaller negative contribution. In addition to the common belief that changes in the electronic structure due to disorder (restoring degeneracies of bands) generally decrease the MAE one can also recall the argument based on spin-orbit coupling induced by Pd: in the ordered sample the interior Fe atoms have eight nearest-neighbor Pd atoms, whereas in the presence of interdiffusion this number is reduced to $4+4c$ on the average. Interestingly enough, the average number of nearest-neighbor Pd atoms around an interior Fe atom remains constant (actually six) for films grown along the (111) direction. This explains that the contributions to ΔE_b from Fe atoms in the originally pure Fe layers are much less affected by a small interdiffusion for the (111) growth

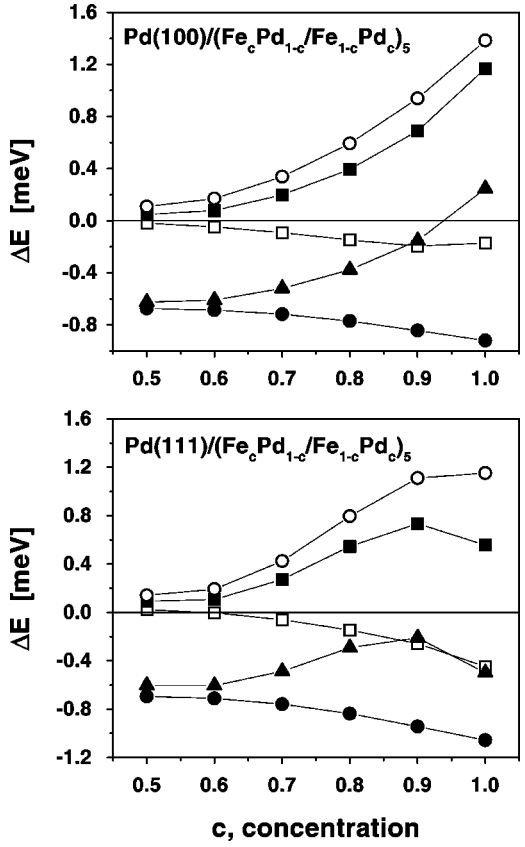

FIG. 6. Band-energy contribution (solid squares), magnetic dipole-dipole energy contribution (solid circles) to the MAE and the total MAE (solid triangles) of interdiffused $(Fe_cPd_{1-c})_5$ films on Pd(100) and Pd(111) substrates. The contributions of the Fe and Pd components in the disordered layers are also shown by open circles and squares, respectively. Solid lines serve as a guide for the eye.

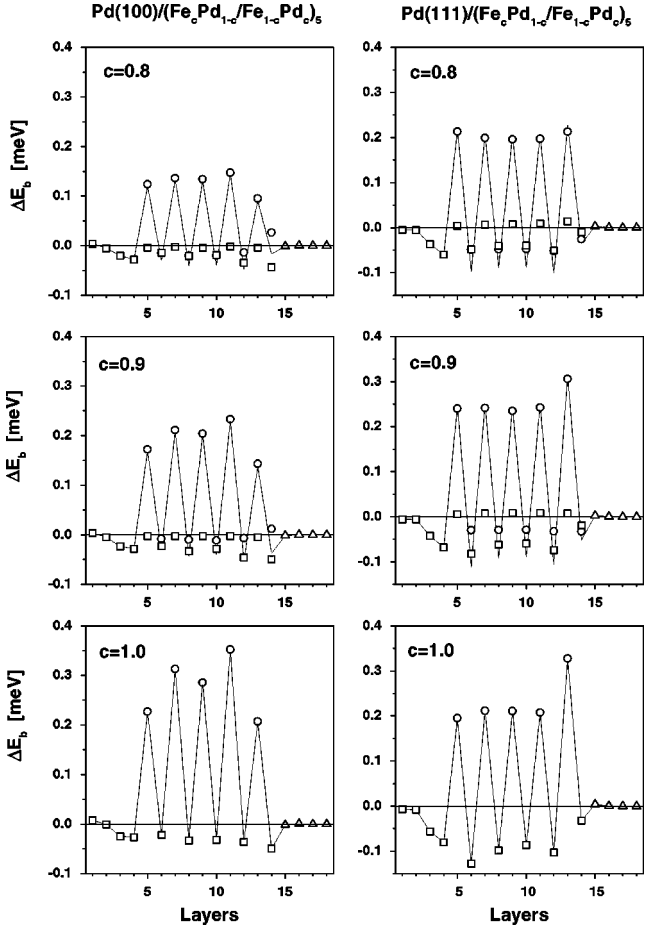

FIG. 7. Layer- and component-resolved contributions (circles, Fe: squares, Pd) to the band-energy part of the MAE in interdiffused $(Fe_cPd_{1-c})_5$ films on Pd(100) and Pd(111) for $c=0.8$, 0.9, and 1. The first four layers correspond to Pd ''buffer'' layers, triangles represent the contributions of empty-sphere layers. Thin solid lines indicate the shape of the total layer-resolved contributions of ΔE_b. The Pd substrate (origin of counting) is to the left, vacuum to the right.

direction—in fact for $c=0.9$ they are even slightly increasing—than those in the case of the (100) growth direction.

IV. CONCLUSIONS

Finally we discuss our results by making comparisons to available experiments and try to answer the question put in the Introduction concerning the mechanism of chemical ordering. The theoretical and computational method used in this paper seems to be so far the only one that has been applied to studying the MAE of realistic thin films and multilayers of disordered alloys. Among the approximations involved, we believe that the most serious one is the neglecting of short-range order and concentration fluctuations that can be particularly important for the 50%-50% alloys. In principle these fluctuations can be taken into account by extending, for example, the method of concentration waves[27,28] to inhomogeneously disordered two-dimensional invariant systems, an approach, which however, would lead to rather complicated mixed partial derivatives of the grand-canonical potential with respect to layer-dependent concentrations.

Regarding merely the band-energy contributions to the MAE (see left upper panel of Fig. 1) our calculated results for Pd(100)/Fe$_n$ are in good qualitative agreement with the experiments of Liu and Bader[7] who for films grown at low temperatures (100 K) observed perpendicular magnetization up to $n\simeq 2.6$ and an in-plane magnetization beyond. By adding ΔE_{dd} the total MAE predicted by theory, however, becomes negative. The most possible reason for this disagreement between theory and experiment is the fact that in our calculations an fcc geometry with the lattice constant of pure Pd was used while in Ref. 7 a bct structure for Fe was deduced. Quite clearly, this structural difference might give rise to pronounced changes both in the band-energy and the shape-anisotropy contributions to the MAE. On the contrary, grown at room temperature (300 K), a strong in-plane anisotropy is found even for ultrathin Fe films on Pd(100),[7,13] which has been related to the ''interface alloying and tetragonalized fct structure.''[13] Our results for an fcc related structure of Pd(100)/$(Fe_{0.5}Pd_{0.5})_n$ (lower left panel of Fig. 1) that shows a tendency for an in-plane magnetization seems to support this experimental finding. Therefore, we

conclude that in this case interface alloying controls the MAE by changing the structure of the Fe films from bct to fct.

For an equiconcentrational FePd alloy deposited onto Pd(100) the $L1_0(100)$ phase is found with magnetization normal to the planes,[17] while at room temperature a disordered γ phase is formed with in-plane magnetization.[16] Our results are consistent with both observations (see left upper panel of Fig. 4 and left lower panel of Fig. 1, respectively). As indicated in terms of the applied interdiffusion scheme (see Fig. 6), in repeated FePd superstructures the change of magnetic moments (shape anisotropy) with respect to chemical ordering does not seem to be essential. We have found that the MAE related to the Fe atoms falls off rapidly with increasing interdiffusion most likely as a consequence of changes in the electronic structure due to disorder, and also via decreased spin-orbit coupling induced by a decreasing amount of nearest-neighbor Pd atoms. Although we have not found corresponding experimental results for Fe and FePd films grown on Pd(111), a comparison to the case of (100) growth direction we made throughout in this work might be interesting from theoretical point of view.

ACKNOWLEDGMENTS

This paper resulted from a collaboration partially funded by the TMR network on ''*Ab-initio* calculations of magnetic properties of surfaces, interfaces, and multilayers'' (Contract No. EMRX-CT96-0089), the RTN network ''Computational Magnetoelectronics'' (Contract No. RTN1-1999-00145), and the Research and Technological Cooperation between Austria and Hungary (OMFB-BMAA, Contract No. A-35/98). Financial support was provided also by the Center of Computational Materials Science (Contract No. GZ-45-451), the Austrian Science Foundation (Contract Nos. P12146 and P12352), and the Hungarian National Science Foundation (Contract Nos. OTKA T030240 and T022609). We also wish to thank the computing center IDRIS at Orsay as part of the calculations was performed on their Cray T3E machine.

[1] A.M. Clogston, B.T. Matthias, M. Pettern, H.J. Williams, E. Corenzwit, and R.C. Sherwood, Phys. Rev. **125**, 541 (1962).
[2] U. Gradmann and R. Bergholz, Phys. Rev. Lett. **52**, 771 (1984).
[3] G.J. Nieuwenhuys, Adv. Phys. **24**, 515 (1975).
[4] A. Oswald, R. Zeller, and P. Dederichs, Phys. Rev. Lett. **56**, 1419 (1986).
[5] C. Binns, C. Norris, G.P. Williams, M.G. Barthes, and H.A. Padmore, Phys. Rev. B **34**, 8221 (1986).
[6] C. Liu and S.D. Bader, Physica B **161**, 253 (1989).
[7] C. Liu and S.D. Bader, J. Vac. Sci. Technol. A **8**, 2727 (1990).
[8] C. Liu and S.D. Bader, J. Magn. Magn. Mater. **93**, 307 (1991).
[9] J. Quinn, Y.S. Li, H. Li, D. Tian, F. Jona, and P.M. Marcus, Phys. Rev. B **43**, 3959 (1991).
[10] F. Pan, T. Yang, J. Zhang, and B.X. Liu, J. Phys.: Condens. Matter **5**, L507 (1993).
[11] A. Boufelfel, R.M. Emrick, and C.M. Falco, Phys. Rev. B **43**, 13 152 (1991).
[12] J. Vogel, A. Fontaine, V. Cros, F. Petroff, J.P. Kappler, G. Krill, A. Rogalev, and J. Goulon, Phys. Rev. B **55**, 3663 (1997).
[13] C. Boeglin, H. Bulou, J. Hommet, X. Le Cann, H. Magnan, P. Le Fèvre, and D. Chandesris, Phys. Rev. B **60**, 4220 (1999).
[14] V. Cros, F. Petroff, J. Vogel, A. Fontaine, J.L. Menéndez, A. Cebollada, W. Grange, J.P. Kappler, M. Finazzi, and N. Brookes, Europhys. Lett. **49**, 807 (2000).
[15] A.V. dos Santos and C.A. Kuhnen, Solid State Commun. **95**, 537 (1995).
[16] P. Kamp, A. Marty, B. Gilles, R. Hoffmann, S. Marchesini, M. Belakhovsky, C. Boeglin, H.A. Dürr, S.S. Deshi, G. van der Laan, and A. Rogalev, Phys. Rev. B **59**, 1105 (1999).
[17] V. Gehanno, A. Marty, B. Gilles, and Y. Samson, Phys. Rev. B **55**, 12 552 (1997).
[18] L. Szunyogh, B. Újfalussy, and P. Weinberger, Phys. Rev. B **51**, 9552 (1995); for a review see P. Weinberger and L. Szunyogh, Comput. Mater. Sci. **17**, 414 (2000).
[19] S.H. Vosko, L. Wilk, and M. Nusair, Can. J. Phys. **58**, 1200 (1980).
[20] P. Weinberger, P.M. Levy, J. Banhart, L. Szunyogh, and B. Újfalussy, J. Phys.: Condens. Matter **8**, 7677 (1996).
[21] P. Weinberger, Philos. Mag. B **75**, 509 (1997).
[22] C. Uiberacker, J. Zabloudil, P. Weinberger, L. Szunyogh, and C. Sommers, Phys. Rev. Lett. **82**, 1289 (1999).
[23] H.J.F. Jansen, Phys. Rev. B **59**, 4699 (1999).
[24] J. Zabloudil, L. Szunyogh, U. Pustogowa, and P. Weinberger, Phys. Rev. B **58**, 6316 (1998).
[25] B. Ujfalussy, L. Szunyogh, and P. Weinberger, in *Properties of Complex Inorganic Solids*, edited by A. Gonis, A. Meike, and P.E.A. Turchi (Plenum Press, New York, 1997), p. 181.
[26] L. Szunyogh, B. Újfalussy, and P. Weinberger, Phys. Rev. B **55**, 14 392 (1997).
[27] S.S.A. Razee, J.B. Staunton, F.J. Pinski, B. Ginatempo, and E. Bruno, Phys. Rev. Lett. **82**, 5369 (1999).
[28] S.S.A. Razee, J.B. Staunton, B. Ginatempo, E. Bruno, and F.J. Pinski, Phys. Rev. B (to be published).